J. Chem. Sci. Vol. 129, No. 10, October 2017, pp. 1647–1657.
DOI 10.1007/s12039-017-1377-0
© Indian Academy of Sciences

REGULAR ARTICLE

The noncovalent complexes of nido-$C_4B_2H_6$ with H_2O, CH_3 OH and NH_3 Lewis bases: A Theoretical study

NAHID ZARE and ABEDIEN ZABARDASTI*
Department of Chemistry, Lorestan University, Khorramabad, Iran
E-mail: zebardasti@yahoo.com

MS received 21 June 2017; revised 13 September 2017; accepted 14 September 2017; published online 14 October 2017

Abstract. Quantum chemical calculations at the MP2/6-311++G(2d,2p) level of theory were used to examine the complexes resulting from the interactions between $C_4B_2H_6$ and HY Lewis bases (HY = NH_3, H_2O, and CH_3OH molecules). Four different directional geometries could be obtained for $C_4B_2H_6$-HY complexes.The complexes with conformation A had (B11-H12$\cdots$H-Y) dihydrogen bond and C-H^{meta}...YH hydrogen bond interactions. In structure B, HY from the pentagonal basal plane interacted with carborane molecule. In conformation C, HY had DHB and HB interactions with peripheral B-H and C-H^{ortho} bonds of the carborane backbone. Finally, conformation D had only hydrogen bond interaction between HY with C-H^{meta} bonds of the $C_4B_2H_6$. Among all the complexes resulting from the interaction of HY with $C_4B_2H_6$, the greatest interaction energy belonged to the complexes with configurations B. The Bader's Quantum Theory of Atoms in Molecules (QTAIM) was used to analyze the optimized complexes. Molecular electrostatic potentials (MEP), vibrational frequencies and molecular energies (HOMO and LUMO) were also calculated for these clusters.

Keywords. Carborane; noncovalent interaction; dihydrogen bond; hydrogen bond; MEP.

1. Introduction

Noncovalent interactions have an important position in crystal packing, molecular recognition, biological procedures and reaction selectivity.[1,2] Hydrogen and dihydrogen bonds are very famous noncovalent interactions, which have attracted much consideration and large amount of experimental and theoretical research.[3–5] The carboranes as important classes in inorganic chemistry are extensively used in synthesis of unique coordination compounds, inorganic pharmaceuticals and biological systems, medicinal chemistry, polymers, especially in boron neutron capture therapy (BNCT).[6–16] Many research studies have commenced to use the unique chemical and physical properties of carboranes for the preparation of novel inorganic pharmaceuticals and biological probes. An interesting overview of $C_4B_2H_6$ activities can be described through its intermolecular interactions including hydrogen bond (HB) and dihydrogen bond (DHB) with other molecules. Nido-$C_4B_2H_6$ is one of the most carbon-rich carboranes that has a pentagonal pyramid structure.[9,17,18] $C_4B_2H_6$ and its derivatives have been the subject of theoretical studies, molecular and electronic structure calculations, dipole moment and ionization potential.[19–21] Nido-$C_4B_2H_6$ (Scheme 1) has Cs point group that exhibits four types of hydrogens. The H5 and H12 are two kinds of hydrogens which are directly attached to the boron atoms ($B^{+\sigma}$–$H^{-\sigma}$), thus known as hydride hydrogens. Also, H6, 9 (meta-Hs) and H7, 8 (ortho-Hs) are two other types of hydrogen atoms attached to the carbon atoms. Due to positive charge, ($C^{-\sigma}$–$H^{+\sigma}$) C-H acts as a hydrogen bond donor toward HY molecules ($H^{+\sigma}$–$Y^{-\sigma}$...$H^{+\sigma}$–$C^{-\sigma}$). In contrast, in the case of the B–H bonds, because of the presence of negative charge on the hydrogen atoms, DHB with HY molecules ($B^{+\sigma}$–$H^{-\sigma}$...$H^{+\sigma}$–$Y^{-\sigma}$) is expected.[16] On the other hand, the presence of different sites for interaction in $C_4B_2H_6$, makes it an adequate nominate for interaction with other molecules. The aim of this study is to investigate the types and relative strengths of the probable interactions that exist between $C_4B_2H_6$ with HY molecules.

*For correspondence

Electronic supplementary material: The online version of this article (doi:10.1007/s12039-017-1377-0) contains supplementary material, which is available to authorized users.

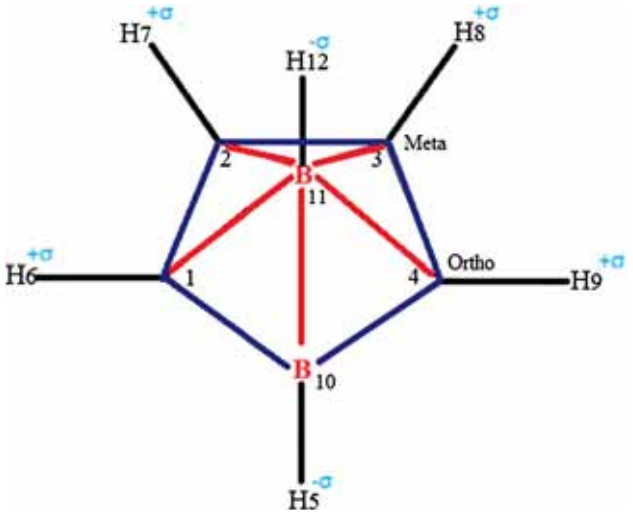

Scheme 1. Schematic representation of $C_4B_2H_6$ structure.

2. Computational

The isolated monomers and complexes were fully optimized at the MP2/6-311++G(2d,2p) theoretical level.[22–26] For all the optimized structures, frequency calculations were performed to determine that all complexes are in their equilibrium structures. The counterpoise approach designed by Bernardi and his co-workers was performed to correct the values of the interaction energies in light of the basis set superposition error (BSSE).[27,28] The AIM 2000 package was used to perform the topological integrations for the subsequent achievement of the QTAIM descriptors.[29,30] The MEP analysis was carried out at the MP2/6-311++G(2d,2p) level of theory by using the Gaussian 03 package.[31] The HOMO-LUMO energy gaps indicated the stability and chemical activities of the compounds.[32–34]

3. Results and Discussion

3.1 *$C_4B_2H_6$–H_2O complexes*

The interaction of $C_4B_2H_6$ with H_2O leads to the formation of adducts denoted as W1, W2, W3 and W4 (Figure 1). In the W1 complex, H_2O had DHB interaction with B-H in the climax and also HB interaction with C-H^{meta} of the carborane molecule. In the DHB interaction within this compound, the H_2O molecule acted ashydrogen bond donor (HBD) and the B-H bond of $C_4B_2H_6$ as hydrogen bond acceptor (HBA); while, in the HB interaction, the H_2O molecule and the C-H^{meta} of $C_4B_2H_6$ acted respectively as HBA and HBD.

In the W2 complex, the H_2O molecule in the bottom of the pyramid interacted with the peripheral bonds of the carborane, leading to the non-classical HB interactions with C-C and B-C bonds of $C_4B_2H_6$(OH_2…C-C and OH_2…B-C), in which the B-C and C-C bonds of the $C_4B_2H_6$ had the HBA role and H_2O had the HBD role.

On the other hand, the W3 structure is a bifurcated complex in which H_2O has DHB interaction with the peripheral B10-H5 bond and HB interaction with C-H^{ortho} of the carborane molecule. According to Figure 1 and Table 1, this combination has the least stability compared with other $C_4B_2H_6$- H_2O adducts. It seems that the ability of the B-H in the climax and C-H^{meta} to form DHB and HB, respectively, is better than peripheral B-H and C-H^{ortho}. The stabilities of the studied complexes shows that B11–H12 actsas a better HBA than B10–H5 does for the intermolecular interactions.

The W4 is a HB complex obtained from the intermolecular interaction of H_2O with H8 atom (H_2O… H8-C3) in the backbone of the $C_4B_2H_6$. In this complex, the oxygen atom of H_2O acted as HBA and the C3-$H8^{meta}$ bond of $C_4B_2H_6$ as HBD. As a result, it can be inferred that depending on the type of the interactions and the stability of the complexes, those complexes which have non-classical interactions with peripheral bonds are stronger than the classical HB interactions, and also HB interactions are stronger than DHB interactions. Therefore, the stabilities of $C_4B_2H_6$–H_2O complexes can be given in the following order: W2 > W4 > W1 > W3.

According to Table S1 (Supplementary Information) and Figure 1, O-H bond lengths are 0.958Å in the free H_2O molecule which show elongation in $C_4B_2H_6$–H_2O adducts. Of course, due to the direct compensation of O-H13 in interaction with carborane, there was a greater bond lengthening in O-H13 than in O-H14.The maximum bond elongationin O-H13 (0.005 Å) occured inW2 which hadthe maximum stabilization energy between $C_4B_2H_6$–H_2O adducts. In addition, there wasa good relationship between the interaction energy and the elongation of O-H bonds. Also, producing the $C_4B_2H_6$–H_2O adducts were accompanied with bond lengths variation in the $C_4B_2H_6$ molecule. For example, in W1,B11-H12 and C2-C3 bonds showed elongation, while C2-H7 and C3-H8 showed contraction upon complex formation. These changes were resulted from the charge transfers from σ_{B-H} to σ^*_{O-H} orbital in the DHB and from $\sigma\, c_{2-}c_3$ to σ^*_{O-H14} orbital in HB interactions.

In the W2 complex, the H atom of H_2O molecule interacted with the peripheral B-C and C-C bonds in the backbone of the $C_4B_2H_6$. As Table S1 (in Supplementary Information) shows B10-C1 and C1-C2 bonds have considerable lengthening, while C2-C3 and C4-B10 bonds show contraction, and C3-C4 bond remains unchanged with complex formation.

In the W3 complex, there were bond lengthening in B10-H5 and C1-H6 and bond shortening in B10-C1 with adduct formation. Finally, in the W4 complex, the $C_4B_2H_6$ bonds were affected less by the intermolecular interactions than the previously mentioned systems.

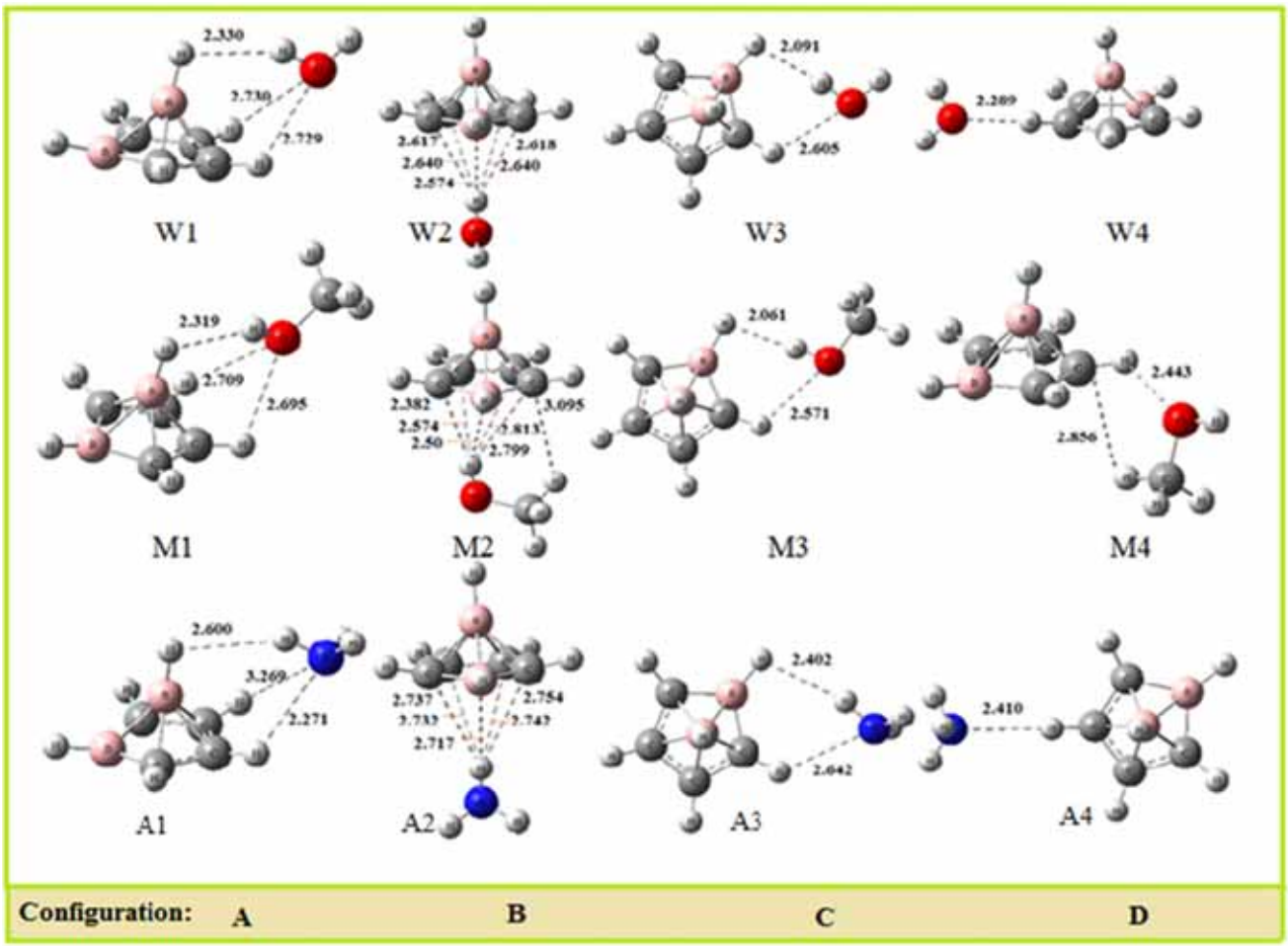

Figure 1. Schematic representation of $C_4B_2H_6$ complexes optimized at MP2/6-311++G(2d, 2p) level.

Table 1. SE^{uncorr}, BSSE, ΔZPE in (kcal.mol^{-1}) calculated at MP2/6-311++G(2d, 2p) level.

Complex	SE^{uncorr}	BSSE	ΔZPE	SE^{cp}	SE^{corr}
W1	−3.49	0.8	11.11	−1.57	−2.37
W2	−4.70	1.38	1.07	−2.25	−3.63
W3	−3.31	1.38	1.15	−0.78	−2.16
W4	−2.88	0.69	0.78	−1.41	−2.50
A1	−2.82	0.64	0.68	−1.50	−2.14
A2	−3.54	1.08	0.73	−1.73	−2.81
A3	−2.72	0.58	0.81	−1.33	−1.91
A4	−3.22	0.62	0.81	−1.79	−2.41
M1	−3.95	0.98	0.67	−2.30	−3.28
M2	−5.84	1.80	0.73	−3.31	−5.01
M3	−3.68	0.90	0.72	−2.06	−2.96
M4	−3.98	0.90	0.63	−2.45	−3.35

$SE^{corr} = \Delta ZPE + SE^{uncorr}$
$SE^{cp} = SE^{corr} + BSSE$

Also, the W2 complex, with the greatest stabilization energy had the most bond length variations. These bond length variations are in line with the relative stabilities of the complexes.

The selected vibrational stretching frequencies (cm^{-1}) with their corresponding intensities (km.mol^{-1}) for H_2O and $C_4B_2H_6$ free molecules as well as their complexes are listed in Table S2 (Supplementary Information). In all the $C_4B_2H_6$–H_2O complexes, the H–O bands showed red shift compared to the isolated H_2O. These red shifts for W1, W2, W3 and W4 complexes were: −29, −51, −33 and −15 cm^{-1}, respectively. This shows that the greatest and the smallest red shifts are observed for W2 and W4 complexes, respectively.

For the W1 complex, C2-H7 and C3-H8 stretching frequencies showed blue shift but B11-H12 and C2-C3 bonds showed red shift with complex formation. Stretching resonance frequencies for C1-B10-C4 and C1…C4 bonds in the W2 complex showed small red shift, while stretching frequency for B10-H5 and B11-H12 showed small blue shift in comparison with the free $C_4B_2H_6$. In the W3 complex, B10-H5 bond showed −33 cm^{-1} red shift while C1-H6 and B11-H12 bonds showed small blue shift with complex formation. It can be concluded that those B-H bonds involved in the interaction show red shift, while the other bonds show

blue shift with complex formation. Finally, in the W4 complex, B10-H5, B11-H12 and C3-H8 bonds showed red shift, while C1-C2 and C2-C3 showed blue shift with complex formation. The results of this study are in agreement with the ambidentate characteristics of $C_4B_2H_6$ through the presence of the multi donor acceptor sites on its backbone which can contribute as Lewis acid or Lewis base centers for intermolecular interactitons.

According to the above discussions on $C_4B_2H_6$–H_2O systems, it can be inferred that the peripheral B–C and C–C bonds, such as HBA, have the strongest interaction with the target molecules. Therefore, from different models considered for the interaction of $C_4B_2H_6$ with H_2O molecules, it can be suggested that the complexes involving peripheral B–C and C–C bonds have the greatest stabilities.

3.2 $C_4B_2H_6$–CH_3OH complexes

The association of $C_4B_2H_6$ with CH_3OH led to the formation ofM1, M2, M3 and M4 complexes (configurations A to D in Figure 1). The M1 complex is a bifurcated complex in which $C_4B_2H_6$ has DHB and HB interactions with CH_3OH molecule. B11-H12 with the O-H of CH_3OH had DHB interaction while the C-H^{meta} bonds (C2-H7 and C3-H8) of $C_4B_2H_6$ such as HBD did HB interaction (bifurcated HB) with the O atom of CH_3OH such as HBA. In the M2 complex, CH_3OH molecule had non-classical HB interactions with the peripheral C-C and B-C bonds of $C_4B_2H_6$. Also, in the M3 complex two types of interactions were observed, B10-H5 had DHB interaction with O-H, while C1-H6 formed HB interaction with the O atom of CH_3OH. Finally, the M4 complex had a HB interaction between the C3-H8 and O-H groups of CH_3OH and also an interaction between the B-C3 of carborane with the H atom of CH_3OH methyl group. According to Table 1, the stabilities of $C_4B_2H_6$–CH_3OH complexes are in this order: M2 > M4 > M1 > M3.

The results showed that the non-classical HB bond between these molecules was stronger than their DHB and HB interactions. Therefore, M2 was the most stable complex in this series. The results further showed different tendencies of B–H and C–H bonds in $C_4B_2H_6$ for intermolecular interactions with CH_3OH. The stabilities of the studied complexes indicated that B11–H12 had a better HBA than B10–H5 did for intermolecular interactions. Apparently, the proximity of B10–H5 to the peripheral B–C and C-C bonds diminishes its charge and makes it a weaker HBA for noncovalent interactions.

O-H bond length was 0.958Å in the isolated CH_3OH molecule which showed 0.001−0.005Å elongation in $C_4B_2H_6$-CH_3OH adduct (Table S1 in Supplementary Information). Among $C_4B_2H_6$-CH_3OH compounds, the M2 complex had the greatest increase of O-H bond length. Similarly, the carborane part of the $C_4B_2H_6$-CH_3OH system underwent considerable bond variations (Table S1 in Supplementary Information). In the M1 complex, B11-H12, C3-H8 and C2-C3 bonds had elongations, while C2-H7 had a small contraction. For M2, data given in Table S1 (Supplementary Information) are showing that B-B bond has the most contraction while C1-B10 has considerable elongation. These variations suggest that those parts of $C_4B_2H_6$ that are closer to CH_3OH (due to the existence of the stronger intermolecular interactions) show larger changes. In the M3 complex, B-B bond had the greatest shortening, while B10-H5 had the greatest lengthening among the $C_4B_2H_6$-CH_3OH complexes. Furthermore, B10-C1 showed small contraction, while B11-C1, B11-C2, B11-C3, B11-C4 showed elongation for the M3 adducts. Finally, in the M4 cluster, all peripheral C-C and B-C bonds of $C_4B_2H_6$ showed elongation among which C1-C2 bond had the greatest lengthening. Furthermore, B10-H5 and B11-H12 bonds increased with complex formation.

The selected vibrational stretching frequencies (cm^{-1}) with their corresponding intensities ($km.mol^{-1}$) for $C_4B_2H_6$-CH_3OH systems are listed in Table S2 (Supplementary Information). In these complexes, the H–O bond shows red shift upon complex formation. These red shifts for the M1, M2, M3 and M4 complexes are in the order: −34, −81, −42 and $-10cm^{-1}$, respectively. As it is evident, the maximum and minimum red shifts belong to the M2 and M4 clusters, respectively. A good correlation can also be found between the stabilities of adducts and their frequency variations in the M4 system.

In the M1 complex, the stretching frequencies of the B11-H12 and B10-H5 showed −28 and $-2cm^{-1}$ red shift; that is to say, B11-H12 bond has a greater shift and as a result a better contribution in the intermolecular interactions. Similarly, other bonds (C2-H7, C3-H8, and C2-C3) that were less involved in the interaction with CH_3OH showed no significant red shift with complex formation. According to Table S2, the stretching frequencies of B-H bonds in the M2 cluster showed 9 and 5 cm^{-1} blue shift. B-B bond in all $C_4B_2H_6$-CH_3OH systems (M1, M2, M3 and M4) showed blue shift among which the one related to the M2 complex was greater. Therefore, based on these results, it can be understood that there is a good relationship between the stretching frequencies and B-B bond lengths. In the M2 complex, also, the stretching frequencies of C1…C4, C1-C2 and C2-C3 bonds showed red shift upon complex formation. In the M3 adduct, B10-H5 bond showed $-36\ cm^{-1}$ red

shift but B11-H12 and B-B bonds showed blue shift with respect to their original bands. Therefore, it can be concluded that B-H bond involved in the interaction showed red shift, while the other one showed blue shift. Eventually, in the M4 cluster, C1-H6 and C3-H8 bonds showed 2 cm^{-1} blue shift, while C2-H7, C4-H9, B10-H5 and B11-H12 bonds showed red shift with respect to their original bands. These results confirm the presence of several sites on the $C_4B_2H_6$ backbone which can act as Lewis acid or Lewis base in the interaction with CH_3OH molecule.

3.3 *$C_4B_2H_6$–NH_3 complexes*

According to Figure 1, depending on the orientation of interactions, the interaction of $C_4B_2H_6$ with ammonia gives four different geometries including A1, A2, A3 and A4 clusters. In the A1 complex, a dihydrogen bond interaction appeared between the B11-H12 bond of carborane as HBA and H13 of NH_3 as HBD (H12…H13) and also a HB interaction between the C3-H8 and N atom of ammonia. In the A2 complex, NH_3 molecule interacted with the pentagonal base of carborane in which B-C and C-C bonds of the $C_4B_2H_6$ acted as HBA and NH_3 as HBD. Similar to the A1, in the A3 complex, DHB interaction was formed between NH_3 molecule and B10-H5 bond and HB interaction appeared between C1-H6 and the N atom of NH_3. Additionally, for DHB, NH_3 molecule had the role of HBD, while B-H bond acted as HBA. On the other hand, for HB interactions, NH_3 and the peripheral C-H bond of $C_4B_2H_6$ acted respectively as HBA and HBD. The A4 complex was a HB complex obtained from the interaction of NH_3 with the C3-H8 of $C_4B_2H_6$. The stabilities of $C_4B_2H_6$–NH_3 complexes are in this order: A2 > A4 > A1 > A3. N-H13 bond was 1.009 Å in the free NH_3 molecule which showed (0.001-0.003 Å) elongation in the A1 to A4 complexes. It is to be noted that, the largest elongation and the greatest stability belonged to the A2complex. In the A1 complex, B11-H12 and B10-H5 bonds showed elongation among which that B-H bond involved in the interaction had a greater elongation. As Table S1 (Supplementary Information) shows, A2, B-B and B10-C1 bonds have the greatest shortening and elongation, respectively. In addition, for C1-C2, C3-C4 and C4-B10, small bond lengthening are observed.

The A3 complex is a bifurcated complex in which NH_3 has a DHB interaction with B10-H5 and a HB interaction with C1-H6. The results showed that, in this cluster, C3-H8 and C3-C4 bonds did not change by intermolecular interactions, while B10-H5 and B-B bonds showed, respectively, the greatest elongation and contraction. Finally, among all the carborane bonds in the A4 complex, C1-B11, C2-B11 and B-B illustrated contraction, C3-H8 had the greatest elongation and the rest showed a small lengthening.

The stretching frequencies and absorption intensities of the $C_4B_2H_6 \cdots NH_3$ complexes are organized in Table S2. According to this table, it can be figured out that although N-H bond lengths do not have considerable changes with complex formation, their stretching frequencies have significant downward shifts (−13 to −28 cm^{-1}). Also, an efficient correlation can be found between the vibrations of the bond lengths and the stretching frequencies of B-H and B-B bonds. On the other hand, the red or blue shifts might be directly in agreement with the increasing and decreasing of the bond lengths. In the A1 complex, the values of −7, −7 and −8 cm^{-1} and 4 cm^{-1} which belong to B10-H5, B11-H12, C3-H8 and B-B bonds, respectively, might be directly consistent with the increasing and decreasing the bond lengths. In the A2 cluster, the B-B, B10–H5 and B11-H12 bonds showed small blue shift, while sym-C1-B10-C4 and C1…C4 resonance frequency showed small red shift. In contrast, C2-C3 and C2-H7 bonds showed small blue shift with complex formation. In the A3 complex, compared to their original bands, B10–H5 showed −21 cm^{-1} red shift, while B-B bond showed 4 cm^{-1} blue shift. On the other hand, unlike other similar complexes such as H_2O and CH_3OH (W3 and M3), in this complex, the stretching frequency of B11-H12 bond did not show any change with complex formation. Eventually, in the A4 cluster, the greatest red shift and the greatest blue shift belonged to (C4-H9, C2-H7) and (C1-C2,C2-C3) sets, respectively. Furthermore, C1-H6 and C3-H8 bonds showed small red shifts with complex formation. In this cluster, also, B10-H5 and B11-H12 bonds had red shifts with complex formation. According to the above discussions on $C_4B_2H_6$–NH_3 systems, it can be concluded that the peripheral B–C and C–C bonds such as HBA had the strongest HB interactions with the target molecules such as HBD. Therefore, as a result of different models with regard to the interaction of $C_4B_2H_6$ with NH_3 molecule, it can be said that the most stable complexes involve in theinteractions with theperipheral B–C and C–C bonds.

3.4 *AIM and MEP analysis*

In order to fulfill one of the objectives of this study, the AIM arguments were used to analyze the characteristics of the intermolecular interactions through the bond critical points (bcp) location (see Figure 2). The electronic density (p), Laplacian ($\nabla^2 p$) parameters and the ratios between the kinetic (Gc) and potential (Vc) electron energy density [1] derived from the Bader theory indicated

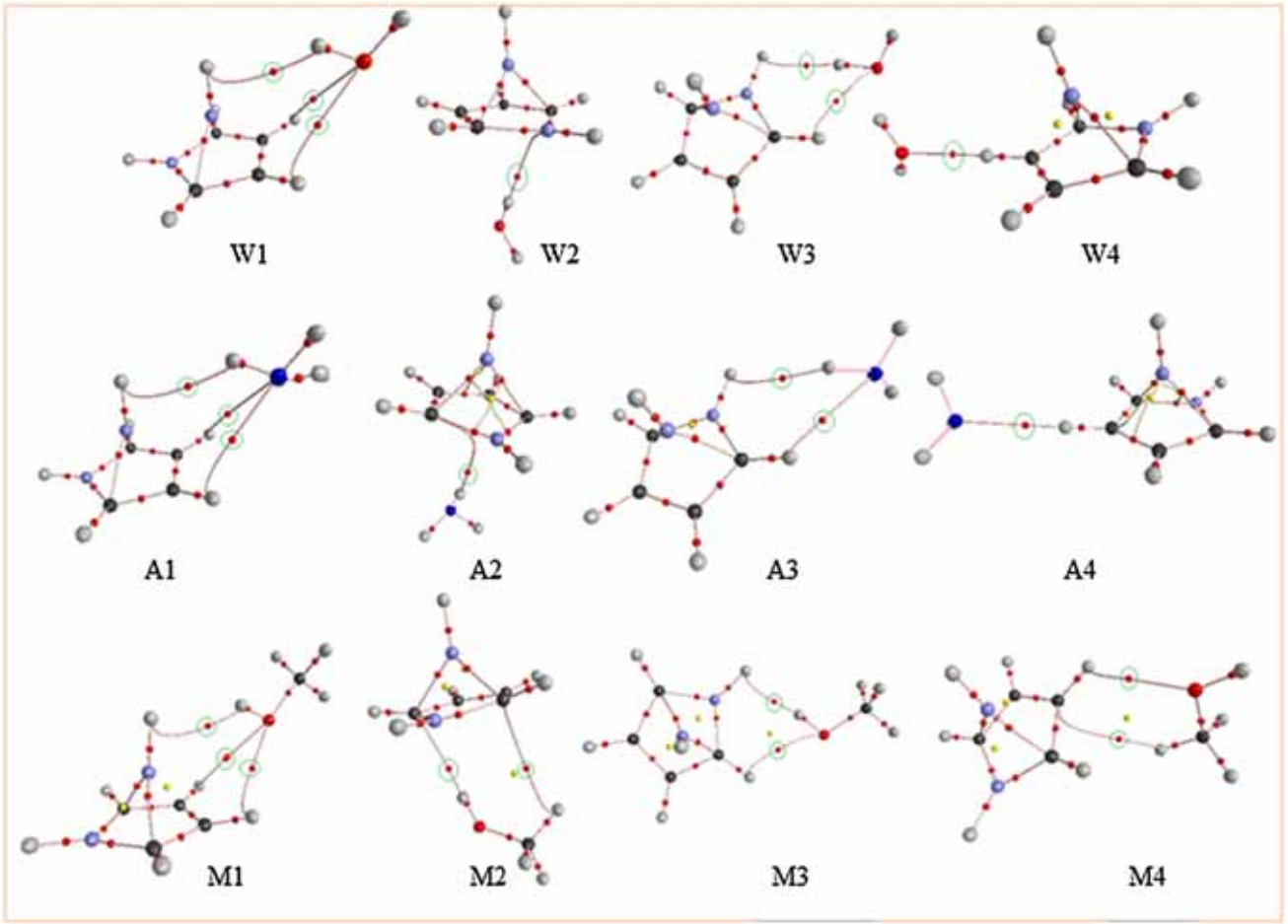

Figure 2. Bond paths (BP) and bond critical points for the complexes obtained from AIM integrations.

Table 2. Topological parameters for fully optimized systems analyzed at MP2/6-311++G(2d, 2p).

Cluster	Bond	ρ	$\nabla^2\rho$	$-G_C$	V_C	$-G_C/V_C$	H_C
W1	H12…H13	0.0066	−0.0231	0.0047	0.0036	1.3006	−0.0011
	O…H7	0.0064	−0.0248	0.0052	0.0042	1.2379	−0.0010
	O…H8	0.0064	−0.0249	0.0052	0.0042	1.2377	−0.0010
W2	H13…B10	0.0097	−0.0305	0.0066	0.0056	1.1845	−0.0010
W3	H5...H13	0.0097	−0.0319	0.0068	0.0056	1.2072	−0.0012
	H6…O	0.0073	−0.0298	0.0063	0.0051	1.2355	−0.0012
W4	H8…O	0.0122	−0.0426	0.0094	0.0082	1.1485	−0.0012
A3	N…H6	0.0102	−0.0332	0.0072	0.0061	1.1793	−0.0011
A2	C1…H13	0.0078	−0.0256	0.0054	0.0044	1.2231	−0.0010
A1	H12…H13	0.0054	−0.0190	0.0038	0.0028	1.3467	−0.0010
	H7…N	0.0081	−0.0268	0.0057	0.0046	1.2240	−0.0010
A4	H8…N	0.0125	−0.0355	0.0079	0.0069	1.1414	−0.0010
M1	H12…H13	0.0069	−0.0234	0.0048	0.0038	1.2728	−0.0010
	H7…O	0.0070	−0.0260	0.0056	0.0047	1.1980	−0.0009
	H8…O	0.0070	−0.0261	0.0056	0.0047	1.1976	−0.0009
M2	C1…H14	0.0147	−0.0161	0.0032	0.0024	1.3332	−0.0008
	H13…C1	0.0135	−0.0409	0.0093	0.0080	1.1355	−0.0011
M3	H13…H5	0.0108	−0.0340	0.0074	0.0064	1.1630	−0.0010
	H6…O	0.0080	−0.0323	0.0069	0.0056	1.2143	−0.0012
M4	C3…H14	0.0058	−0.0199	0.0040	0.0030	1.3127	−0.0010
	O…H8	0.0100	−0.0370	0.0080	0.0068	1.1827	−0.0012

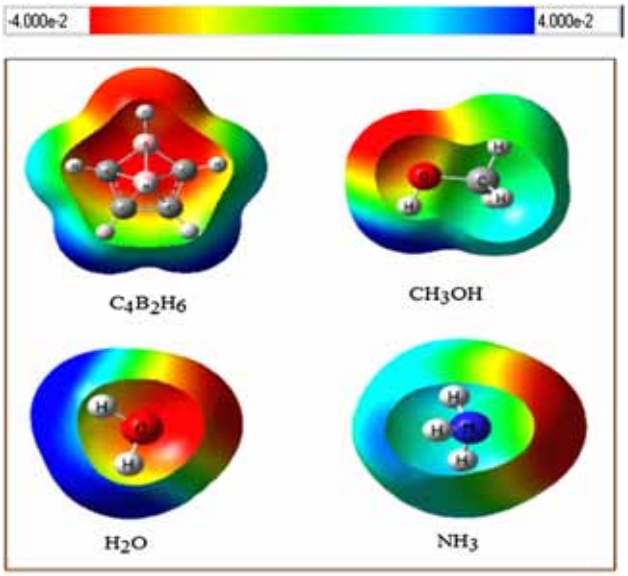

Figure 3. MP2/ 6-311++G (2d, 2p). Calculated 3D molecular electrostatic potential contour map of ($C_4B_2H_6$, H_2O, CH_3OH and NH_3). The red color shows the minimal molecular electrostatic potential and the blue color denotes the maximal molecular electrostatic potential.

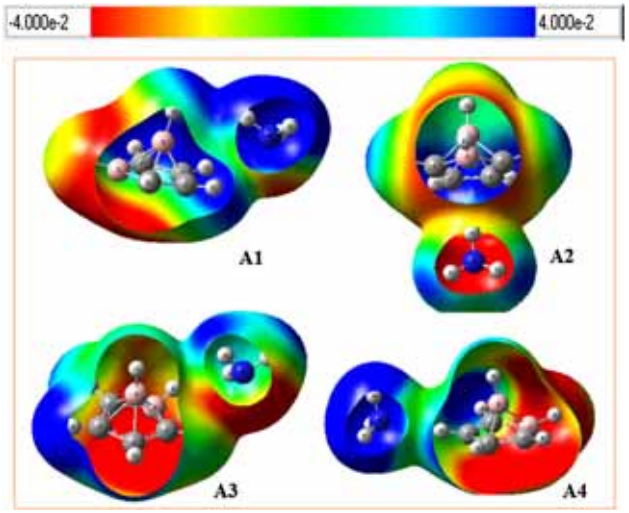

Figure 4. MP2/ 6-311++G(2d,2p), calculated 3D molecular electrostatic potential contour map of $C_4B_2H_6$ … NH_3. The red color represents the minimal molecular electrostatic potential and the blue color denotes the maximal molecular electrostatic potential.

the type of interactions. As indicated in Table 2, the AIM calculations shows that both H · · · N, H. . .O and H · · · H bonds have little charge density; therefore, it can be proved that the interactions are essentially of the non-covalent type. The positive values of $\nabla^2 p$ in Table 2 highlights the fact that all HBs are of closed-shell type interactions. Figures 3 and 4 represent the MEP profiles for $C_4B_2H_6$, CH_3OH, H_2O and NH_3 monomers as well as $C_4B_2H_6$-NH_3 complexes (MEP profiles for the $C_4B_2H_6$-CH_3OH and $C_4B_2H_6$-H_2O clusters are shown in Figures S1 and S2, Supplementary Information). These figures show that a negative region of the electrostatic potential is located on the pentagonal base of the $C_4B_2H_6$. There is also a negative zone (B11-H12) for the interaction with HY molecules at the climax of the pyramid. Thus, in DHB and non-classical HB interactions, HY had HBD role and B-H, C-C and B-C bonds of $C_4B_2H_6$ had HBA roles. In contrast, in HB interactions, the O and N atoms of HY acted as HBA and C-H (Ortho and Meta) of the pentagonal base of the $C_4B_2H_6$ acted as HBD.[41,42]

3.5 *HOMO–LUMO analysis*

HOMO and LUMO are very important parameters[35–37] for chemical reactions. One can determine the way the molecule interacts with other species. Hence, they are called the Frontier orbitals. The highest occupied molecular orbital (HOMO) and the lowest unoccupied molecular orbital (LUMO) are considered as important parameters in quantum chemistry. The energy of the frontier orbitals of molecules is related to the energy of ionization (IE) and electron affinity, which are calculated according to Koopman's theorem.[38]

$$-E_{HOMO} = IE \quad (1)$$

$$-E_{LUMO} = EA \quad (2)$$

Also, the absolute electronegativity (χ_{abs}) and absolute hardness (η) are related to IA and EA[39] as given below:

$$\chi_{abs} = (IE + IA)/2 = (E_{HOMO} + E_{LUMO})/2 \quad (3)$$

$$\eta = (IE - IA)/2 = (E_{HOMO} - E_{LUMO})/2 \quad (4)$$

A molecule with a small frontier orbital gap is more polarizable and is generally associated with a high chemical reactivity and low kinetic stability and is also termed as soft molecule while as hard molecules have a large HOMO-LUMO gap.[40]

The HOMO indicates the ability to donate an electron and the LUMO shows the ability to obtain an electron.[41] In order to evaluate the energetic behavior of these compounds, the HOMO LUMO energy calculations were done by means of MP2 method using 6-311++G(2d,2p) basis set. Figure 5 shows the HOMO and LUMO frontier molecular orbitals along with their related energies for $C_4B_2H_6$-NH_3 structures. Also,the information about Frontier orbital's HOMO and LUMO for $C_4B_2H_6$-CH_3OH and $C_4B_2H_6$-H_2O Compounds with their corresponding energies are shown in Figures S3 and S4 (Supplementary Information). The positive and negative phases are portrayed in red and green colors, respectively. Details of the frontier molecular orbitals in

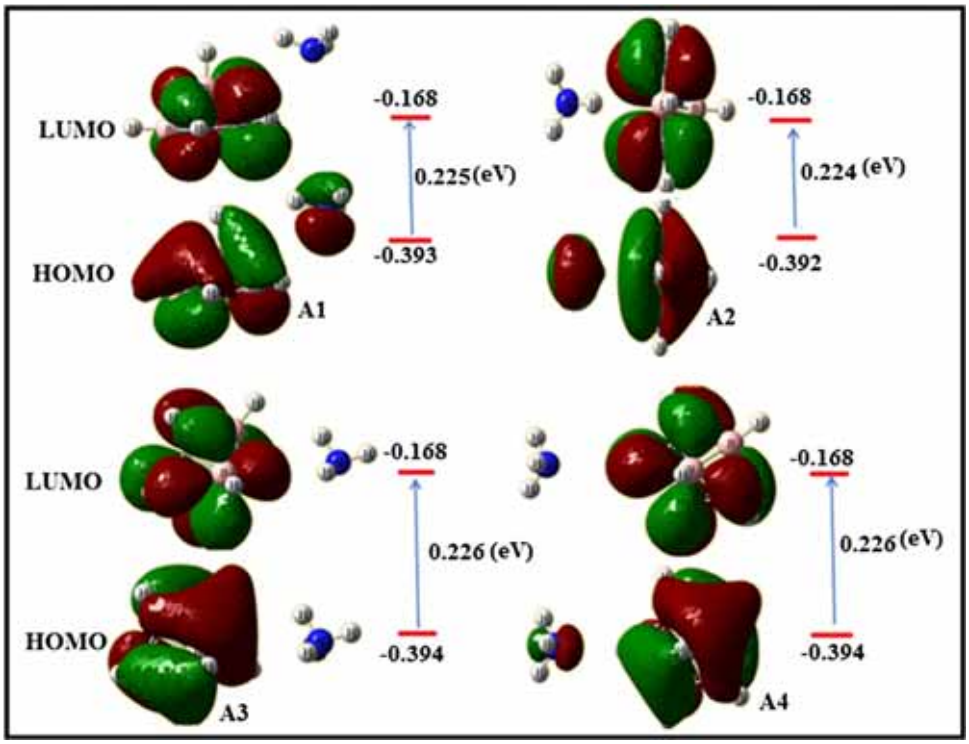

Figure 5. Frontier orbitals HOMO and LUMO of the $C_4B_2H_6$-NH_3 compounds with their corresponding energies (eV).

Table 3. HOMO and LUMO energies, HOMO–LUMO energy gap, absolute electronegativity (χ_{abs}) and absolute hardness (η) (eV) for $C_4B_2H_6$ …HY (HY = NH_3, H_2O, CH_3OH) complexes.

	W1	W2	W3	W4	A1	A2	A3	A4	M1	M2	M3	M4
HOMO	−0.394	−0.395	−0.394	−0.394	−0.393	−0.392	−0.394	−0.394	−0.385	−0.385	−0.383	−0.385
LUMO	−0.168	−0.168	−0.168	−0.168	−0.168	−0.168	−0.168	−0.168	−0.168	−0.168	−0.168	−0.168
$\Delta E_{HOMO-LUMO}$	0.226	0.227	0.226	0.226	0.225	0.224	0.226	0.226	0.217	0.217	0.215	0.217
IE	0.394	0.395	0.394	0.394	0.393	0.392	0.394	0.394	0.385	0.385	0.383	0.385
AE	0.168	0.168	0.168	0.168	0.168	0.168	0.168	0.168	0.168	0.168	0.168	0.168
χ_{abs}	0.281	0.281	0.281	0.281	0.280	0.280	0.281	0.281	0.276	0.276	0.275	0.276
η	0.113	0.113	0.113	0.113	0.112	0.112	0.113	0.113	0.108	0.108	0.107	0.108

the dimers are presented in Table 3. The $\Delta E_{HOMO-LUMO}$ for $C_4B_2H_6$-H_2O complexes are ordered as: 0.226, 0.227, 0.226, and 0.226 (eV) for W1, W2, W3 and W4 complexes, respectively. These results show that the greatest $\Delta E_{HOMO-LUMO}$ is related to the W2 complex, which has the most stable energy. The remaining clusters have the same chemical activity. Similarly, the values of $\Delta E_{HOMO-LUMO}$ for $C_4B_2H_6$-CH_3OH clusters are ordered as: 0.217, 0.217, 0.215 and 0.217 (eV) for M1, M2, M3 and M4 clusters, respectively. In terms of chemical activity, the M3 cluster has the most activity. According to Figure 5 and Table 3, the value of $\Delta E_{HOMO-LUMO}$ in $C_4B_2H_6$-NH_3 complexes is as follows: 0.225, 0.224, 0.226, and 0.226 (eV) for A1, A2, A3 and A4, respectively. Consequently, according to Table 3, the maximum and minimum amount of $\Delta E_{HOMO-LUMO}$ are observed for $C_4B_2H_6$-H_2O and $C_4B_2H_6$-CH_3OH clusters, respectively. Also, from another perspective, the frontier orbitals can be studied. In the clusters of $C_4B_2H_6$-H_2O and $C_4B_2H_6$-NH_3, the highest percentage of HOMO and LUMO orbitals are focused on the carborane molecule, while in all the $C_4B_2H_6$-CH_3OH clusters, HOMO orbitals are concentrated on the CH_3OH molecule and LUMO orbitals are focused on the carborane molecule.

3.6 *The comparison of the complexes*

In most cases, the complexes derived from the interaction of these Lewis bases (CH_3OH, NH_3 and H_2O) with $C_4B_2H_6$ exhibited similar behavior. For example, in all three categories of clusters, the W1, M1 and A1 clusters showed the greatest elongation of B11-H12 bond

(0.003, 0.003, 0.001 Å). On the other hand, among all the intermolecular interactions, dihydrogen bonding was the most important one which resulted in the formation of these adducts. In the A2, M2 and W2 clusters, the greatest change was observed for B-B bond length. That is, all B-B bonds underwent shortening (the length of B-B bond in A2, M2 and W2 are −0.005, −0.006 and −0.007 Å, respectively). The results showed that there is a good correlation between the B-B bond length decreasing and the B-B frequency increasing (7, 13, 12 cm^{-1} blue shift for A2, M2 and W2 clusters). Also, in the bifurcated complexes (A3, W3, M3), the greatest bond elongation occurred for their B10-H5 bond (0.002, 0.003, 0.004 Å) that showed a good correlation with the red shift of their stretching frequencies (−21, −33, −36 cm^{-1}). Moreover, in all groups, only W4, M4 and A4 (HB complexes) had the greatest elongations (0.001, 0.001, 0.003 Å) for C3-H8 bonds. Finally, among all the complexes obtained from the interaction of $C_4B_2H_6$ with HY molecule, only W2, M2 and A2, or those complexes in which HY molecule had a nonclassical HB interaction from the pentagonal base of $C_4B_2H_6$, had the greatest stability in each group.

4. Conclusions

Ab initio MP2/6-311++G(2d,2p) calculations were carried out on $C_4B_2H_6$…HY systems. $C_4B_2H_6$ could have intermolecular interactions with HY (HY = H_2O, CH_3OH and NH_3) molecules. For the interaction of $C_4B_2H_6$ with HY molecules, H-bond and DHB-bond, complexes were obtained. The results showed that, $C_4B_2H_6$–CH_3OH dimers were more stable than $C_4B_2H_6$–H_2O and $C_4B_2H_6$–NH_3, and that was because of the greater dipole moment of CH_3OH compared to H_2O and NH_3. Also, according to the different models of interactions (conformers A, B, C and D), it can be said that those complexes which include the peripheral B–C and C–C bonds as electron donor had the greatest stabilities in the three systems. The following statements are confirmed from the results of this study: a) Complexes with configuration A had C1 symmetry composed of DHB and HB intermolecular interactions. HBs had a positive effect on dihydrogen bonds and vice versa. b) Configuration B complexes had interactions with all bonds of the carborane skeleton except the B-H bond in the climax. The nonclassical bonds in these complexes were unique and the transfer of electrons from the orbital σ of C-B or C-Cbonds to the σ* orbital of HY molecule was the main factor of their stability. These were $\sigma - \sigma$ nonclassical bonds indicating that the σ system of one molecule interacted with the σ* system of the other. c) Third group of complexes (complexes with configuration C) were less stable than those with configuration A. As it was explained in (a), HBs had a positive effect on dihydrogen bonds. It can be concluded that the more the number of hydrogen bonds in a complex, the more stable it is. d) As observed for configurations D, these complexes were composed of only one hydrogen bond. In other words, σ electron donation by C-H to the σ* orbital of HY molecule was the main factor of their stability. Moreover, the existence the electropositive substituent (methyl group in CH_3OH) also had a stabilizing interaction between the H atom of the CH_3 group of CH_3OH and C-H^{meta} of $C_4B_2H_6$. This, in turn, helped the stability of the M4 complex compared to their counterpart complexes (A4 and W4) in other configurations. e) With regard to the energy gaps, $C_4B_2H_6$–CH_3OH clusters had the most chemical activities. In contrast, $C_4B_2H_6$–H_2O complexes which had the least chemical activity were the most stable of complexes.

Supplementary Information (SI)

All additional information pertaining to the minimal molecular electrostatic potential (MEP) profiles, Tables S1, S2, Figures S1-S4, Frontier orbitals HOMO and LUMO of $C_4B_2H_6$-CH_3OH and $C_4B_2H_6$-H_2O compounds are given in the Supporting Information, available at www.ias.ac.in/chemsci.

References

1. Zabardasti A, Talebi N, Kakanejadifard A and Saki Z 2014 The B–C and C–C bonds as preferred electron source for H-bond and Li-bond interactions in complex pairing of $C_4B_2H_6$ with HF and LiH molecule *Struct. Chem*. DOI 10.1007/s11224-015-0586-8
2. Zabardasti A, Arabpour M and Zare N 2013 Theoretical studies ointermolecular interactions of arachnopentaborane (11) with HF and LiH *Comput. Theor. Chem*. **1008** 27
3. Grimes R N 2011 In *Carboranes* 2nd edn. (London: Academic Press) p. 1170
4. Pasinski J P and Beaudet R A 1947 Microwave spectrum, structure, and dipole moment of 2,3,4,5-tetracarbahexaborane(6) *Chem. Phys*. **61** 683
5. Dewar Michael J S, Jie C and Zoebisch E G 1988 AM1 calculations for compounds containing boron *Organometallics* **7** 513
6. Epstein I R, Tossell J A, Switkes E, Stevens R M and Lipscomb W N 1971 Hexaborane (10): self-consistent fieldwavefunction, localized orbitals and relationships to chemical properties *Inorg. Chem*. **10** 171
7. Tian S X 2005 Theoretical study of isoelectronic molecules: B_6H_{10}, 2-CB_5H_9, 2, 3-$C_2B_4H_8$, 2, 3, 4-$C_3B_3H_7$, and 2,3,4,5- $C_4B_2H_6$ *Phys. Chem. A* **109** 6580

8. Gill W R, Jones M E, Wade K, Porterfield W and Wong E H 2005 Stability patterns in borane cluster chemistry rationalized bymextended Hückel molecular orbital studies *J. Mol. Struc- Theochem.* **261** 161
9. Hofmann M, Fox M A, Greatrex R, Schleyer P V R and Williams R E 2001 Empirical and ab initio energy/architectural patterns for 73 nido-6 \V[-carborane isomers, from B(6)H(9)(-) to C(4)B(2)H(6) *Inorg. Chem*. **40** 1790
10. Larsen A S, Holbrey J D, Tham F S and Reed C A 2000 *J. Am. Chem. Soc.* **122** 7264
11. Pindado G J, Lancaster S J, Thornton-Pett M and Bochmann M 1998 *J. Am. Chem. Soc*. **120** 6816
12. Reed A C 1998 Carboranes: A new class of weakly coordinating anions for strong electrophiles, oxidants, and superacids *Accounts Chem. Res*. **31** 133
13. Curtis M A, Finn M G and Russell N G 1998 A hydridotantalum (V)-carborane analogue of Schwartz's reagent: synthesis and reactivity *J. Organomet. Chem*. **550** 469
14. Blandford I, Jeffery J C, Jelliss P A and Stone F G A 1998 Synthesis and Crystal Structure of the Novel Dianion $[Re(CO)_3(\eta 5 - 7 - CB10H11)]^{2-}$. Reactions with Platina and Palladaphosphin Chlorides *Organometallic* **17** 1402
15. Felekidis A, Goblet-Stachow M, Liegeois J F, Pirotte B, Delarge J, Demonceau A, Fontaine M, Noels A F, Chizhevsky I T, Zinevich T V, Bregadze V I, Dolgushin F M, Yanovsky A I and Struchkov Y T 1997 Ligand effects in the hydrogenation of methacycline to doxycycline and epi-doxycycline catalysed by rhodium complexes molecular structure of the key catalyst [closo-3, 3-(η 2, 3-$C_7H_7CH_2$)-3, 1, 2 − $RhC_2B_9H_{11}$] *J. Organomet. Chem*. **405** 536
16. Chizhevsky I T and Struchkov A I 1997 Semisandwich platinum metals metallacarboranes derived from nido-$C_2B_9H_{12}^-$: Chemistry and structural studies. *J. Organomet. Chem.* **536** 51
17. Teixidor F, Flores M A, Vinas C, Kivekas R and Sillanpa R 1996 [Rh (7-SPh-8-Me-7, 8-$C_2B_9H_{10}$) (PPh_3)$_2$]: A New Rhodacarborane with Enhanced Activity in the Hydrogenation of 1-Alkenes *Angew. Chem. Int. Edit*. **35** 2251
18. Chizhevsky I T, Pisareva I V, Petrovskii P V, Bregadze V I, Dolgushin F M, Yanovsky A I, Struchkov Y T and Hawthorne M F 1996 Synthesis and Molecular Structure of a Novel Monocarbon Hydridorhoda carborane: closo-2, 7-(PPh_3) 2-2-H-2-Cl-1-(NMe_3)-2, 1-$RhCB_{10}H_9$ *Inorg. Chem*. **35** 1386
19. Hawthorne M F and Maderna A 1999 Applications of radiolabeled boron clusters to the diagnosis and treatment of cancer *Chem. Rev*. **99** 3421
20. McLemore D K, Dixon D A and Strauss S H 1999 Density functional theory and fluorocarboranes: I. Trends in B- H and B- F distances and dissociation energies for $CB_{11}H_{12}$- nFn- anions (n= 0, 1, 6, 11) *Inorg. Chim. Acta* **294** 193
21. Ivanova S M, Ivanov S V, Miller S M, Anderson O P, Solntsev K A and Strauss S H 1999 Mono-, di-, tri-, and tetracarbonyls of copper (I), including the structures of Cu $(CO)_2$ (1-Bn-$CB_{11}F_{11}$) and $[Cu(CO)_4][1\text{-Et-}CB_{11}F_{11}]$ *Inorg. Chem*. **38** 375
22. Jiang W, Chizhevsky I T, Mortimer M D, Chen W, Knobler C B, Johnson S E, Gomez F A and Hawthorne M F 1996 Macrocyclic Compounds Composed of Carborane Icosahedra Linked by Organic Bridging Groups *Inorg. Chem*. **35** 5417
23. Arterburn J B and Quintana Wu Y W 1996 Synthesis and characterization of a new isocyanato carborane anion $[7\text{-O-C-N-7-CB10H12}]^-$; study on its reactivity toward amino containing compounds *Polyhedron* **15** 4355
24. Plesek J 1992 Potential applications of the boron cluster compounds *Chem. Rev.* **92** 269
25. Westerhausen M, Guckel C, Schneiderbauer S, Noth H and Hosmane N S 2001 The First Barium–Carborate Complex: Synthesis and Structural Investigation *Angew. Chem. Int. Edit.* **40** 1902
26. Patmore N J, Mahon M F, Steed J W and Weller A S 2001 Synthesis and characterisation of Mo (η-L)$(CO)_3$+(η-L = C_5H_5 or C_5Me_5) fragments ligated with $[CB_{11}H_{12}]^-$ and derivatives. Isolation and structural characterisation of an intermediate in a silver salt metathesis reaction *J. Chem. Soc., Dalton Trans.* **3** 277
27. Vyakaranam K Li S, Zheng C and Hosmane N S 2001 Substituent effect on the carborane coupling reaction: synthesis and crystal structure of 1-phenyl-2-[2,3-benzobicyclo (3,3,0)-1 oxo-4-oxa-7-aza-8-yl]-1, 2-dicarba-closo-dodecaborane (12) *Inorg. Chem. Commun*. **4** 180
28. Rockwell J J, Herzog A, Peymann T, Knobler C B and Hawthorne M F 2000 Recent advances in the field of camouflaged carboranes and polyhedral boranes *Curr. Sci.* **78** 405
29. Herzog A, Knobler C B, Hawthorne M F, Maderna A and Siebert W 1999 Camouflaged Carboranes as Surrogates for C (60): Syntheses of Functionalized Derivatives by Selective Hydroxyalkylation *J. Org. Chem*. **64** 1045
30. Li F, Shelly K, Knobler C B and Hawthorne M F 1999 The Synthesis of $[Me_4N]_2$ [a_2 − $B20H_{16}$ $(NH_3)_2$] and trans-$B_{20}H_{16}$ $(NH_3)_2$ from $[Me_3NH][cis\text{-}B_{20}H_{17}NH_3]$ and Their Structural Characterization *Inorg. Chem*. **38** 4926
31. Frisch M J, TrucksG W, Schlegel H B, Scuseria G E, Robb M A, Cheeseman J R, Montgomery J A, Vreven T, Kudin K N, Burant J C, Millam J M, Iyengar S S, Tomasi J, Barone V, Mennucci V B, Cossi M, Scalmani G, Rega N, Petersson GA, Nakatsuji H, Hada M, Ehara M, Toyota K, Fukuda R, Hasegawa J, Ishida M, Nakajima T, Honda Y, Kitao O, Nakai H, Klene M, Knox J E, Hratchian H P, Cross J B, Adamo C, Jaramillo J, Gomperts R, Tratmann S R E, Yazyev O, Austin AJ, Cammi R, Pomelli C, Ochterski JW, Ayala PY, Morokuma K, Voth GA, Salvador P, Dannenberg J J, Zakrzewski V G, Dapprich S, Daniels A D, Strain M C, Farkas O, Malick D K, Rabuck A D, Raghavachari K, Foresman J B, AOrtiz J, Cui Q, Baboul A G, Clifford S, Cioslowski J, Stefanov B B, Liu G, Liashenko A, Piskorz P, Komaromi I, Martin R L, Fox D J, Keith T, Al-Laham M A, Peng C Y, Nanayakkara A, Challacombe M, Gill P M W, Johnson B, Chen W, Wong M W, Gonzalez C and Pople J A 2003 *GAUSSIAN 03. Gaussian Inc, Pittsburgh*
32. Teixidor F, Gomez S, Lamrani M, Vinas C, Sillanpaeae R and Kivekaes R 1997 Mixed Cobaltacarboranes Incorporating η5-Pyrrolyl and Dicarbollide Ligands.

Synthetic Routes, Structures and Mechanistic Implications *Organometallics* **16** 1278
33. Rousseau R, Lee S, Canadell E, Teixidor F, Vinas C and Stibr B 1996 Proposed mechanism for the isomerization of the first parent tricarbollide, [nido-7, 8, 9-$C_3B_8H_{11}$]-, to [nido-7, 8, 10-$C_3B_8H_{11}$]$^-$ *New J. Chem.* **20** 277
34. Zheng Z, Knobler C B and Hawthorne M F 1997 Recognition of electron-donating guests by carborane supported multidentate macrocyclic Lewis acid hosts: mercuracarborand chemistry *Accounts Chem. Res.* **30** 267
35. Zabardasti A, Kakanejadifard A, Hoseini A S and Solimannejad M 2010 Competition between hydrogen and dihydrogen bonding: interaction of B_2H_6 with CH_3OH and $CHnX_3$-nOH derivatives *J. Chem. Soc. Dalton Trans.* **39** 5918
36. Zabardasti A, Goudarziafshar H, Salehnassaj M and Oliveira Boaz G 2014 A computational study of hydrogen bonds in intermolecular systems of high complexity: arachno pentaborane(11)$\cdots$Y *J. Mol. Model.* **20** 240
37. Zabardasti A and Sharifi-Rad A 2016 A new approach on diminutive effects for non-covalent interactions: fused bicyclic hydrogen-bonded complexes of hypohalous acids with fluoromethanol *Mol. Phys.* **114** 3341
38. Maurya R C, Malik B A, Mir J M, Vishwakarma P K, Rajak D K and Jain N 2015 Mixed ligand cobalt(II) complexes of bioinorganic and medicinal relevance, involving dehydroacetic acid and b-diketones: Their synthesis, hyphenated experimental- DFT, thermal and bactericidal facets *J. Mol.Struct.* **1099** 266
39. Ebenso E, Arslan T, Kandemirli F, Love I, Saracoglu M and Umoren S A 2010 Theoretical studies of some sulphonamides as corrosion inhibitors for mild steel in acidic medium *Int. J. Quantum. Chem.* **110** 2614
40. Pearson R G 1993 The principle of maximum hardness *Acc. Chem. Res.* **26** 250
41. Zabardasti A, Sharifi-Rad A and Kakanejadifard A 2015 Interplay between H$\cdots$O, H$\cdots$X, X$\cdots$O and X$\cdots$X interactions in the complex pairing of formyl halides with hypohalous acids *Spectrochim. Acta A* **151** 746
42. Cheng J, Li R, Li Q, Jing B, Liu Z, Li W, Gong B and Sun J 2010 Prominent Effect of Alkali Metals in Halogen-Bonded Complex of MCCBr-NCM$\prime$(M and M$\prime$ = H, Li, Na, F, NH_2, and CH_3) *J. Phys. Chem. A* **114** 10320